

An Enhanced iUPQC for Improve Voltage Regulation in Micro Grid Applications

Chenigaram Manjula

M.Tech Student,
JB Institute of Technology,
Telangana, India.

Pasam Venubabu

Assistant Professor,
JB Institute of Technology,
Telangana, India.

Fathima Azra

HoD
JB Institute of Technology,
Telangana, India.

Abstract

This paper proposes an enhanced controller for the dual topology of the unified power quality conditioner (iUPQC) extending its applicability in power-quality compensation, as well as in micro grid applications. By using this controller, beyond the conventional UPQC power quality features, including voltage sag/swell compensation, the iUPQC will also provide reactive power support to regulate not only the load-bus voltage but also the voltage at the grid-side bus.

In other words, the iUPQC will work as a static synchronous compensator (STATCOM) at the grid side, while providing also the conventional UPQC compensations at the load or micro grid side. In the improved iUPQC controller, the currents synthesized by the series converter are determined by the average active power of the load and the active power to provide the dc-link voltage regulation, together with an average reactive power to regulate the grid-bus voltage. In this manner, in addition to all the power-quality compensation features of a conventional UPQC or an iUPQC, this improved controller also mimics a STATCOM to the grid bus. The proposed topology realize by using MATLAB/SIMULINK environment. Simulation results are provided to verify the new functionality of the topology.

Index Terms—iUPQC, micro grids, power quality, static synchronous compensator (STATCOM), Multiconverter unified power quality conditioner (MC-UPQC).

INTRODUCTION:

Inexhaustible power of nonlinear loads with a high harmonic distortion voltage utility network, thereby affecting the operation of critical loads. The increasing number of power-electronics-driven loads used generally in the industry has brought about uncommon power quality problems. In contrast, power-electronics-driven loads frequently require ideal sinusoidal supply voltage in order to function properly, whereas they are the most responsible ones for abnormal harmonic currents level in the distribution system. In this scenario, devices that can mitigate these drawbacks have been developed over the years. Some of the solutions involve a flexible compensator, known as the unified power quality conditioner (UPQC) [1]–[7] and the static synchronous compensator (STATCOM) [8]–[13].

The power circuit of a UPQC consists of a combination of a shunt active filter and a series active filter connected in a back-to-back configuration. This combination allows the simultaneous compensation of the load current and the supply voltage, so that the compensated current drawn from the grid and the compensated supply voltage delivered to the load are kept balanced and sinusoidal. The dual topology of the UPQC, i.e., the iUPQC, was presented in [14]–[19], where the shunt active filter acts as an ac-voltage source and the series one as an ac-current source, both at the fundamental frequency. This is a key point to better design the control gains, as well as to optimize the LCL filter of the power converters, which allows improving effectively the overall performance of the compensator [20].

The STATCOM has wide scope in transmission networks to regulate the voltage by means of dynamic reactive power compensation. Nowadays, the STATCOM is largely used for voltage regulation [9], whereas the UPQC and the iUPQC have been selected as solution for more specific applications [21]. Moreover, these last ones are used only in particular cases, where their relatively high costs are justified by the power quality improvement it can provide, which would be unfeasible by using conventional solutions. By joining the extra functionality like a STATCOM in the iUPQC device, a wider scenario of applications can be reached, particularly in case of distributed generation in smart grids and as the coupling device in grid-tied micro grids.

In [16], the performance of the iUPQC and the UPQC was compared when working as UPQCs. The main difference between these compensators is the sort of source emulated by the series and shunt power converters. In the UPQC approach, the series converter is controlled as a non sinusoidal voltage source and the shunt one as a non sinusoidal current source. Hence, in real time, the UPQC controller has to determine and synthesize accurately the harmonic voltage and current to be compensated. On the other hand, in the iUPQC approach, the series converter acts as a controlled sinusoidal current source and the shunt converter as a controlled sinusoidal voltage source. This means that it is not necessary to determine the harmonic voltage and current to be compensated, since the harmonic voltages appear naturally across the series current source and the harmonic currents flow naturally into the shunt voltage source.

This paper proposes an improved controller, which addition the iUPQC functionalities. This improved version of iUPQC controller includes all functionalities of those previous ones, including the voltage regulation at the load-side bus, and now providing also voltage regulation at the grid-side bus, like a STATCOM to the grid. Simulation results are provided to validate the new controller design. This paper is organized in five sections. After this introduction, in

Section II, the iUPQC applicability is explained, as well as the novel feature of the proposed controller. Section III presents the proposed controller and an analysis of the power flow in steady state. Finally, Sections IV and V provide the simulation results and the conclusions, respectively.

Preliminaries of iUPQC

In actual power converters, as the switching frequency increases, the power rate capability is reduced. Therefore, the iUPQC give alternative solutions if compared with the UPQC in case of high-power applications, since the iUPQC compensating references are pure sinusoidal waveforms at the fundamental frequency. Moreover, the UPQC has higher switching losses due to its higher switching frequency.

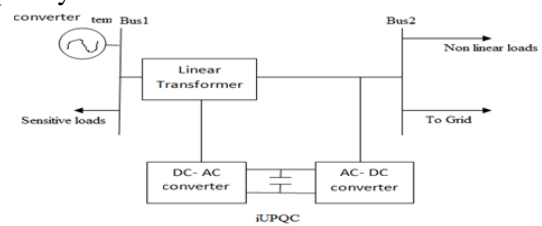


Fig. 1. Block diagram of applicability of iUPQC.

The applicability of the enhanced iUPQC controller, Fig. 1 depicts an electrical system with two buses in spotlight, i.e., bus A and bus B. Bus A is a critical bus of the power system that supplies sensitive loads and serves as point of coupling of a micro grid. Bus B is a bus of the micro grid, where nonlinear loads are connected, which requires premium-quality power supply. The voltages at buses A and B must be regulated, in order to properly supply the sensitive loads and the nonlinear loads. The effects caused by the harmonic currents drawn by the nonlinear loads should be mitigated, avoiding harmonic voltage propagation to bus A.

The scope of a STATCOM to guarantee the voltage regulation at bus A is not enough because the harmonic currents drawn by the nonlinear loads are not mitigated. On the other hand, a UPQC or an iUPQC between bus A and bus B can compensate the

harmonic currents of the nonlinear loads and compensate the voltage at bus B, in terms of voltage harmonics, unbalance, and sag/swell. Nevertheless, this is still not enough to guarantee the voltage regulation at bus A. Hence, to achieve all the desired goals, a STATCOM at bus A and a UPQC (or an iUPQC) between buses A and B should be employed.

An attractive solution would be the use of a modified iUPQC controller to provide also reactive power support to bus A, in addition to all those functionalities of this equipment, as presented in [16] and [18]. Note that the modified iUPQC serves as an intertie between buses A and B. Moreover, the micro grid connected to the bus B could be a complex system comprising distributed generation, energy management system, and other control systems involving micro grid, as well as smart grid concepts [22]. In summary, the modified iUPQC can provide the following functionalities:

- a) “smart” circuit breaker as an intertie between the grid and the micro grid;
- b) energy and power flow control between the grid and the micro grid (imposed by a tertiary control layer for the micro grid);
- c) reactive power support at bus A of the power system;
- d) voltage/frequency support at bus B of the micro grid;
- e) harmonic voltage and current isolation between bus A and bus B (simultaneous grid-voltage and load-current active filtering capability);
- f) voltage and current imbalance compensation.

According to the conventional iUPQC controller, the shunt converter imposes a controlled sinusoidal voltage at bus B; As a result, the shunt converter has no further degree of freedom in terms of compensating active- or reactive-power variables to expand its functionality. On the other hand, the series converter of a conventional iUPQC uses only an active-power control variable p , in order to synthesize a fundamental sinusoidal current drawn from bus A, corresponding to the active power demanded by bus B. If the dc link of the iUPQC has no large energy storage system or even

no energy source, the control variable p also serves as an additional active-power reference to the series converter to keep the energy inside the dc link of the iUPQC balanced. In this case, the losses in the iUPQC and the active power supplied by the shunt converter must be quickly compensated in the form of an additional active power injected by the series converter into the bus B.

The iUPQC can serve as: a) “smart” circuit breaker and as b) power flow controller between the grid and the micro grid only if the compensating active-power and reactive-power references of the series converter can be set arbitrarily. In this case, it is necessary to provide an energy source (or large energy storage) associated to the dc link of the iUPQC.

The last degree of freedom is represented by a reactive-power control variable \bar{q} for the series converter of the iUPQC. In this way, the iUPQC gives reactive-power compensation like a STATCOM to the bus A of the grid. As it will be confirmed, this functionality can be added into the controller without degrading all other functionalities of the iUPQC.

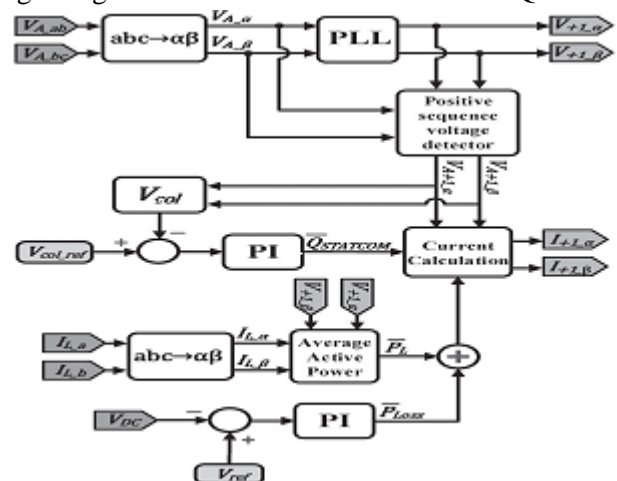


Fig. 2. Novel iUPQC controller.

Enhanced Multi Converter IUPQC Controller

A. Main Controller

The iUPQC hardware and the measured units of a three-phase three-wire system that are used in the controller. Fig. 2 shows the proposed controller. The

controller inputs are the voltages at buses A and B, the current demanded by bus B (iL), and the voltage v_{DC} of the common dc link. The outputs are the shunt-voltage reference and the series-current reference to the pulse width modulation (PWM) controllers. The voltage and current PWM controllers can be as simple as those employed in [18], or be improved further to better deal with voltage and current imbalance and harmonics [23]–[28].

First, the simplified Clark transformation is applied to the measured variables. As example of this transformation, the grid voltage in the $\alpha\beta$ -reference frame can be calculated as

$$\begin{bmatrix} V_{A_ \alpha} \\ V_{A_ \beta} \end{bmatrix} = \begin{bmatrix} 1 & 1/2 \\ 0 & \sqrt{3}/2 \end{bmatrix} \begin{bmatrix} V_{A_ ab} \\ V_{A_ bc} \end{bmatrix} \quad (1)$$

The shunt converter imposes the voltage at bus B. Thus, it is necessary to synthesize sinusoidal voltages with nominal amplitude and frequency. Consequently, the signals sent to the PWM controller are the phase-locked loop (PLL) outputs with amplitude equal to 1 p.u. There are many possible PLL algorithms, which could be used in this case, as verified in [29]–[33].

In the original iUPQC approach as presented in [14], the shunt-converter voltage reference can be either the PLL outputs or the fundamental positive-sequence component V_{A+1} of the grid voltage. The use of V_{A+1} in the controller is useful to minimize the circulating power through the series and shunt converters, under normal operation the grid voltage will be also regulated by the proposed iUPQC. In other words, both buses will be regulated independently to track their reference values.

The series converter synthesizes the current drawn from the grid bus (bus A). In the original approach of iUPQC, this current is calculated through the average active power required by the loads PL plus the power P_{Loss} . The load active power can be estimated by

$$PL = V_{+1_ \alpha} \cdot iL_{_ \alpha} + V_{+1_ \beta} \cdot iL_{_ \beta} \quad (2)$$

where $iL_{_ \alpha}$, $iL_{_ \beta}$ are the load currents, and $V_{+1_ \alpha}$, $V_{+1_ \beta}$ are the voltage references for the shunt converter. A low-pass filter is used to obtain the average active power (PL). The losses in the power converters and the circulating power to provide energy balance inside the iUPQC are calculated indirectly from the measurement of the dc-link voltage. In other words, the power signal P_{Loss} is determined by a proportional– integral (PI) controller (PI block in Fig.2), by comparing the measured dc voltage V_{DC} with its reference value.

The additional control loop to provide voltage regulation like a STATCOM at the grid bus is represented by the control signal $Q_{STATCOM}$ in Fig. 2. This control signal is obtained through a PI controller, in which the input variable is the error between the reference value and the actual aggregate voltage of the grid bus, given by

$$V_{col} = \sqrt{v_{A+1_ \alpha}^2 + v_{A+1_ \beta}^2} \quad (3)$$

The sum of the power signals PL and P_{Loss} composes the active-power control variable for the series converter of the iUPQC (p) described in Section II. Likewise, $Q_{STATCOM}$ is the reactive-power control variable q . Thus, the current references $i_{+1\alpha}$ and $i_{+1\beta}$ of the series converter are determined by

$$\begin{bmatrix} i_{+1_ \alpha} \\ i_{+1_ \beta} \end{bmatrix} = \frac{1}{v_{A+1_ \alpha}^2 + v_{A+1_ \beta}^2} \begin{bmatrix} V_{A+1_ \alpha} & V_{A+1_ \beta} \\ V_{A+1_ \beta} & -V_{A+1_ \alpha} \end{bmatrix} \begin{bmatrix} \bar{P} + \bar{P}_{LOSS} \\ \bar{Q}_{STATCOM} \end{bmatrix} \quad (4)$$

B. Power Flow in Steady State

The following procedure, based on the average power flow, is useful for estimating the power ratings of the iUPQC converters. For combined series–shunt power conditioners, such as the UPQC and the iUPQC, only the voltage sag/swell disturbance and the power factor (PF) compensation of the load produce a circulating average power through the power conditioners [34],

[35]. the compensation of a voltage sag/swell disturbance at bus B causes a positive sequence voltage at the coupling transformer ($V_{series} \neq 0$), shows in Fig. 3 since $V_A \neq V_B$. Moreover, V_{series} and i_{PB} in the coupling transformer leads to a circulating active power P_{inner} in the iUPQC and also, the compensation of the load PF increases the current supplied by the shunt converter. The following analysis is valid for an iUPQC acting like a conventional UPQC or including the extra compensation like a STATCOM.

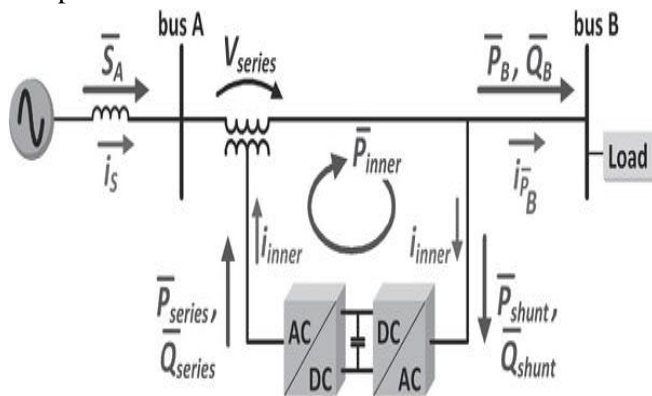


Fig. 3. iUPQC power flow in steady-state.

First, the circulating power will be calculated when the iUPQC is operating just like a conventional UPQC. Afterward, the equations will include the STATCOM functionality to the grid bus A. In both cases, it will be assumed that the iUPQC controller is able to force the shunt converter of the iUPQC to generate fundamental voltage always in phase with the grid voltage at bus A. For simplicity, the losses in the iUPQC will be neglected.

For the first case, the following average powers in steady state can be determined:

$$\bar{S}_A = \bar{P}_B \quad (5)$$

$$\bar{Q}_{shunt} = -\bar{Q}_B \quad (6)$$

$$\bar{Q}_{series} = \bar{Q}_A = 0 \text{ var} \quad (7)$$

$$\bar{P}_{series} = \bar{P}_{shunt} \quad (8)$$

where \bar{S}_A and \bar{Q}_A are the apparent and reactive power injected in the bus A; \bar{P}_B and \bar{Q}_B are the active and reactive power injected in the bus B; \bar{P}_{shunt} and \bar{Q}_{shunt} are the active and reactive power drained by the shunt converter; \bar{P}_{series} and \bar{Q}_{series} are the active and reactive power supplied by the series converter, respectively.

Equations (5) and (8) are derived from the constraint of keeping unitary the PF at bus A. In this case, the current

Passing through the series converter is responsible only for supplying the load active power, that is, it is in phase (or counter phase) with the voltages V_A and V_B . Thus, (7) can be stated. Consequently, the coherence of the power flow is ensured through (8).

If a voltage sag or swell occurs, \bar{P}_{series} and \bar{P}_{shunt} will not be zero, and thus, an inner-loop current (i_{inner}) will appear. The series and shunt converters and the aforementioned circulating active power (P_{inner}) flow inside the equipment. It is convenient to define the following sag/swell factor. Considering V_N as the nominal voltage

$$k_{sag/swell} = \frac{|V_A|}{|V_N|} = \frac{V_A}{V_N} \quad (9)$$

From (5) and considering that the voltage at bus B is kept regulated, i.e., $V_B = V_N$, it follows that

$$\sqrt{3} \cdot k_{sag/swell} \cdot V_N \cdot i_S = \sqrt{3} \cdot V_N \cdot i_{PB}$$

$$i_S = \frac{i_{PB}}{k_{sag/swell}} = i_{PB} + i_{inner} \quad (10)$$

$$i_{inner} = \left| i_{PB} \left(\frac{1}{k_{sag/swell} - 1} \right) \right| \quad (11)$$

The circulating power is given by

$$\bar{P}_{inner} = \bar{P}_{series} = \bar{P}_{shunt} = 3(V_A - V_B) (i_{PB} + i_{inner}) \quad (12)$$

From (11) and (12), it follows that

$$\bar{P}_{inner} = 3(V_N - V_A) \left(\frac{\bar{P}_B}{3V_N} \frac{1}{k_{sag/swell}} \right) \quad (13)$$

$$\bar{P}_{inner} = \bar{P}_{series} = \bar{P}_{shunt} = \frac{1 - k_{sag/swell}}{k_{sag/swell}} \bar{P}_B \quad (14)$$

Thus, (14) demonstrates that \bar{P}_{inner} depends on the active power of the load and the sag/swell voltage disturbance. In order to verify the effect on the power rate of the series and shunt converters, a full load system $S_B = \sqrt{P_B^2 + Q_B^2} = 1 P.U.$ With PF ranging from 0 to 1 was considered. It was also considered the sag/swell voltage disturbance at bus A ranging $k_{sag/swell}$ from 0.5 to 1.5. In this way, the power rating of the series and shunt converters are obtained through (6)–(8) and (14).

Fig. 4 depicts the apparent power of the series and shunt power converters. In these figures, the $k_{sag/swell}$ - axis and the PF-axis are used to evaluate the power flow in the series and shunt power converters according to the sag/swell voltage disturbance and the load power consumption, respectively. The power flow in the series converter indicates that a high power is required in case of sag voltage disturbance with high active power load consumption. In this situation, an increased \bar{P}_{inner} arises and high rated power converters are necessary to ensure the disturbance compensation. Moreover, in case of compensating

sag/swell voltage disturbance with high reactive power load consumption, only the shunt converter has high power demand, since \bar{P}_{inner} decreases. It is important to highlight that, for each PF value, the amplitude of the apparent power is the same for capacitive or inductive loads. In other words, Fig. 4 is the same for \bar{Q}_B capacitive or inductive.

If the iUPQC performs all original UPQC functionalities together with the STATCOM functionality, the voltage at bus A is also regulated with the same phase and magnitude, that is, $\dot{V}_A = \dot{V}_B = \dot{V}_N$, and then, the positive sequence of the voltage at the coupling transformer is zero ($\bar{V}_{series} = 0$). Thus, in steady state, the power flow is determined by

$$\bar{S}_A = \bar{P}_B + \bar{Q}_{STATCOM} \quad (15)$$

$$\bar{Q}_{STATCOM} + \bar{Q}_{series} = \bar{Q}_{shunt} + \bar{Q}_B \quad (16)$$

$$\bar{Q}_{series} = 0 \text{ var} \quad (17)$$

$$\bar{P}_{series} = \bar{P}_{inner} = 0 \text{ W} \quad (18)$$

where $\bar{Q}_{STATCOM}$ is the reactive power that provides voltage regulation at bus A. Ideally, the STATCOM functionality mitigates the inner-loop active power flow (\bar{P}_{inner}), and the power flow in the series converter is zero. Consequently, if the series converter is properly designed along with the coupling transformer to synthesize the controlled currents I_{+1_α} and I_{+1_β} , as shown in Fig.2, then a lower power converter can be employed.

Contrarily, the shunt converter still has to provide the full reactive power of the load and also to drain the reactive power injected by the series converter to regulate the voltage at bus A.

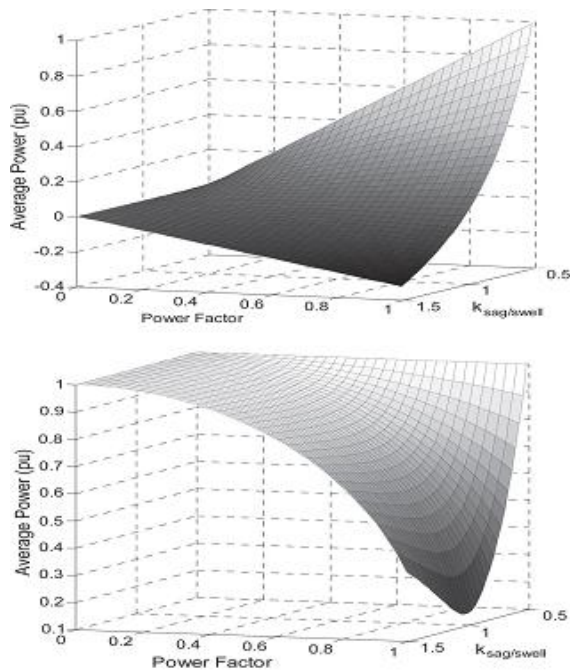


Fig. 4. Apparent power of the series and shunt converters, respectively.

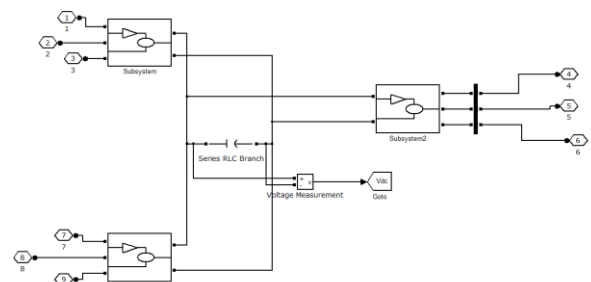


Fig. 6. simulation model of iUPQC subsystem (series & shunt controller)

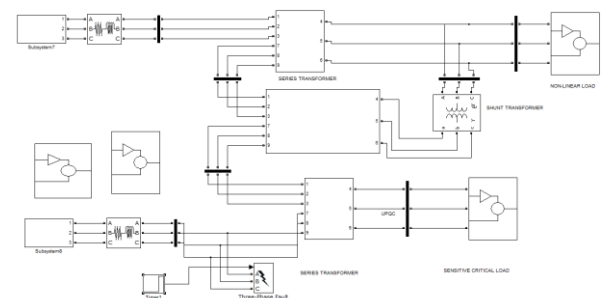


Fig. 7. Simulink model of Multi converter based iUPQC with unbalanced load system

Simulation Results and Discussion:

The proposed topology of iUPQC is developed by using MABLAB-Simulink software to simulate and verify the features as aforementioned in previous sections

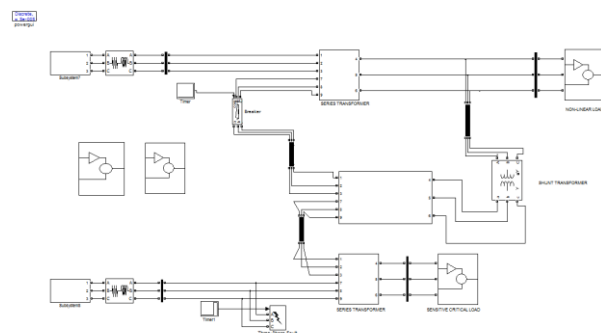


Fig. 5. Simulink model of Multi converter based iUPQC with balanced load system

The series & shunt controllers are designed to implement as the Multiconverter based UPQC (MC-UPQC), this improved features in different operating conditions. The series & shunt controller simulink subsystems are shown in Fig. 6. The proposed model is simulated in balanced and unbalanced load conditions, the putained Fig. 5&7 are respectively.

Distortion and Sag/Swell on the Bus Voltage:

Let us consider that the power system consists of two three-phase three wire 380v, 50-HZ utilities. The BUS1 voltage contains the seventh-order harmonic with a value of 20%, and the BUS2 voltage contains the fifth-order harmonic with a value of 35%. The BUS1 voltage contains 25% sag between $0.1s < t < 0.2s$ and 20% swell between $0.2s < t < 0.3s$. the BUS2 voltage contains 35% sag between $0.15s < t < 0.25s$ and 30% swell between $0.25 < t < 0.3s$. the nonlinear/sensitive load L1 is a three-phase rectifier load which supplies an RC load of 10 and 30F. finally, the critical load L2 contains a balanced RL load of 10 and 100MH.

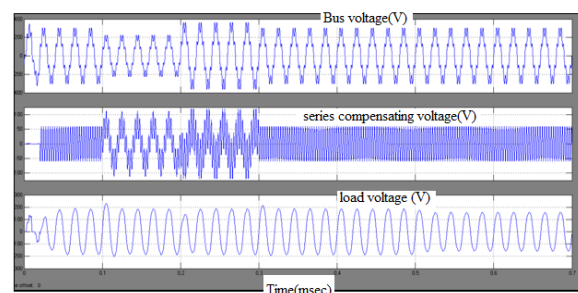


Fig. 8 Bus voltage, series compensating voltage, and load voltage in feeder1.

The MC-UPQC is switched on at $t = 0.02s$. the BUS1 voltage, the corresponding compensation voltage injected by VSC1, and finally load L1 voltage are shown in fig in all figures, only the phase a waveform is shown for simplicity.

Similarly, the BUS2 voltage, the corresponding compensation voltage injected by VSC3, and finally, the load I2 voltage are shown in fig .as shown in these figures, distorted voltages of bus1 and bus2 are satisfactorily compensated for across the loads I1 and I2 with very good dynamic response.

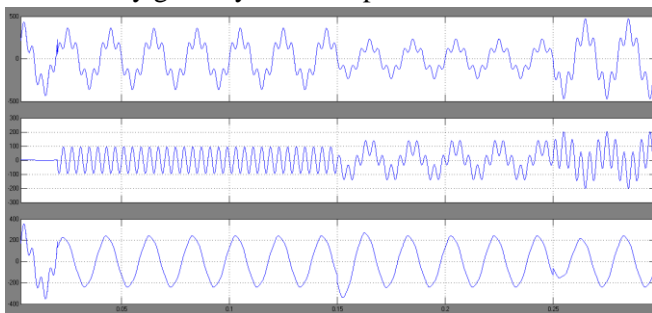


Fig. 9 Bus2 voltage, series compensating voltage, and load voltage in feeder2.

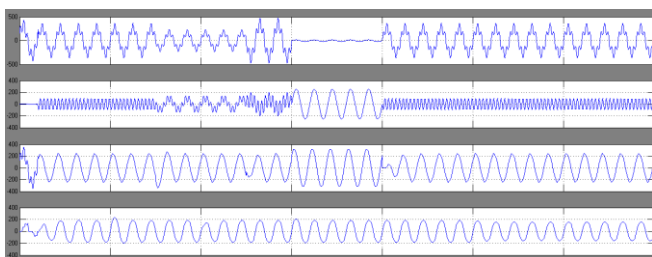


Fig. 10 simulation results for an upstream fault on feeder2: bus2 voltage, compensating voltage, and L1 and L2 voltages.

The nonlinear load current, its corresponding compensation current injected by vsc2, compensated feeder1 current, and, finally, the dc-link capacitor voltage are shown in fig .the distorted nonlinear load current is compensated very well, and the total harmonic distortion (THD) of the feeder current is reduced from 28.5% to less than 5%. Also the dc voltage regulation loop has functioned properly under all disturbances, such as sag/swell in both feeders.

UPSTREAM FAULT ON FEEDER2:

When a fault occurs in feeder2 the voltage across the sensitive/critical load L2 is involved in sag/swell or interruption. This voltage imperfection can be compensated for by VSC2.

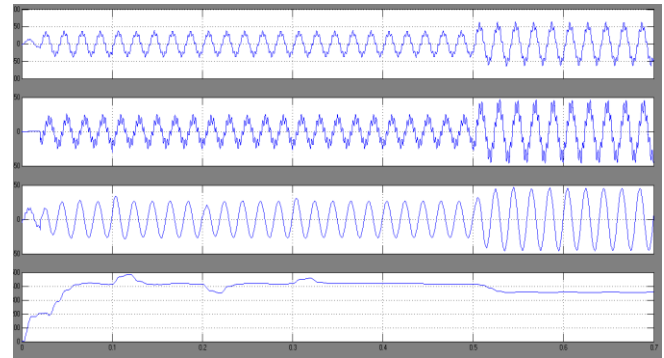


Fig. 11 simulation result nonlinear load current, compensating current, feeder1 and capacitor voltage.

In this case, the power required by load L2 is supplied through VSC2 and VSC3. This implies that the power semi conductor switches of VSC2 and VSC3 must be rated such that total power transfer is possible. This may increase the cost of device, but the benefit that may be obtained can offset the expense.

In the proposed configuration, the sensitive/critical load on feeder2 is fully protected against distortion, sag/swell, and interruption. Furthermore, the regulated voltage across the sensitive load on feeder1 can supply several customers who are also protected against distortion, sag/swell, and momentary interruption.

Therefore, the cost of the MC-UPQC must be balanced against the cost of interruption, based on reliability indices, such as the customer average interruption duration index and customer average interruption frequency index. It is expected that the MC-UPQC cost can be recovered in a few years by charging higher tariffs for the protected lines. The performance of the MC-UPQC under a fault condition on feeder2 is tested by applying a three-phase fault to ground on feeder2 between $0.3s < t < 0.4s$. Simulation results are shown

LOAD CHANGE:

To evaluate the system behaviour during a load change, the nonlinear load L1 is doubled by reducing its resistance to half at $t = 0.5s$. the other load, however, is kept

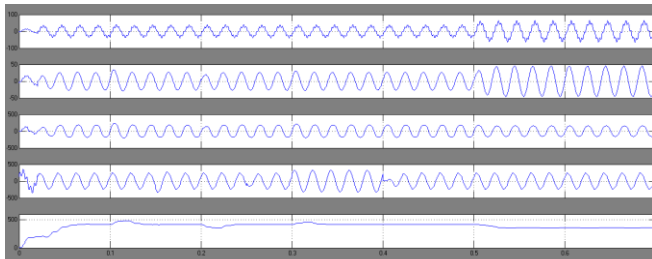


Fig. 12 simulation results for load change: nonlinear load current, feeder1 current, load L1 voltage, and load L2 voltage, and dc-link capacitor voltage unchanged.

The L1 changes, the load voltages $ut1$ and $ut2$ remain undisturbed, the dc bus voltage is regulated, and the nonlinear load current is compensated.

UNBALANCE VOLTAGE:

The control strategies for shunt and series VASCs, which are introduced in sectionII, are based on the d-q method. They are capable of compensating for the unbalanced source voltage and unbalanced load current. To evaluate the control system capability for unbalanced voltage compensation, a new simulation is performed.

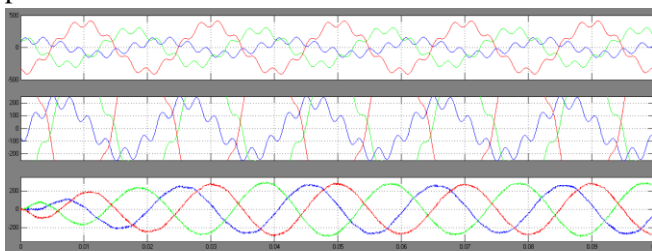


Fig. 13 Bus1 voltage, series compensating voltage, and load voltage in feeder1 under unbalanced source voltage.

In this new simulation, the BUS2 voltage and the harmonic components of BUS1 voltage are similar to those given in sectionIV. however, the fundamental component bBUS1 Voltage is an unbalanced three-

phase voltage with an unbalance factor of 40%. This unbalance voltage is given by

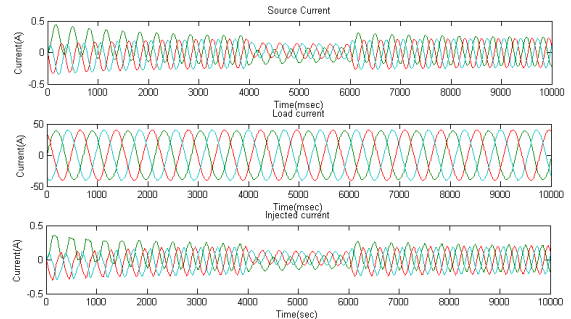


Fig. 14 Simulation results of source Current, load Current & injected Current

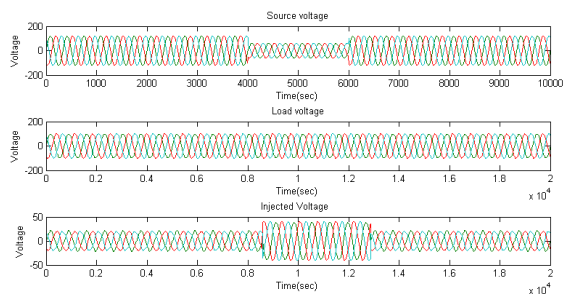


Fig. 15 Simulation results of source voltage, load voltage & injected voltage

The simulation results for the three-phase BUS1 voltage, series compensation voltage, and load voltage in feeder1 are shown in fig .the simulation results show that the harmonic components and unbalance of BUS1 voltage are compensated for by injecting the proper series voltage. In this figure, the load voltage is a three-phase sinusoidal balance voltage with regulated amplitude.

CONCLUSION:

Finally a new configuration for simultaneous compensation of voltage and current in adjacent feeders has been proposed. The new configuration is named multi converter based improved unified power-quality conditioner (iUPQC). Compared to a conventional UPQC, the proposed topology is capable of fully protecting critical and sensitive loads against distortions, sags/swell, and interruption in two-feeder systems. The idea can be theoretically extended to multibus/multifeeders systems by adding more series

Voltage Source Converters. The grid-voltage regulation was achieved with no load, as well as when supplying a three-phase nonlinear load. The performance of voltage regulation at both sides of the iUPQC was improved, even while compensating harmonic current and voltage imbalances.

REFERENCES:

[1] K. Karanki, G. Gedda, M. K. Mishra, and B. K. Kumar, "A modified three-phase four-wire UPQC topology with reduced DC-link voltage rating," *IEEE Trans. Ind. Electron.*, vol. 60, no. 9, pp. 3555–3566, Sep. 2013.

[2] V. Khadkikar and A. Chandra, "A new control philosophy for a unified power quality conditioner (UPQC) to coordinate load-reactive power demand between shunt and series inverters," *IEEE Trans. Power Del.*, vol. 23, no. 4, pp. 2522–2534, Oct. 2008.

[3] K. H. Kwan, P. L. So, and Y. C. Chu, "An output regulation-based unified power quality conditioner with Kalman filters," *IEEE Trans. Ind. Electron.*, vol. 59, no. 11, pp. 4248–4262, Nov. 2012.

[4] A. Mokhtatpour and H. A. Shayanfar, "Power quality compensation as well as power flow control using of unified power quality conditioner," in *Proc. APPEEC*, 2011, pp. 1–4.

[5] J. A. Munoz et al., "Design of a discrete-time linear control strategy for a multicell UPQC," *IEEE Trans. Ind. Electron.*, vol. 59, no. 10, pp. 3797–3807, Oct. 2012.

[6] V. Khadkikar and A. Chandra, "UPQC-S: A novel concept of simultaneous voltage sag/swell and load reactive power compensations utilizing series inverter of UPQC," *IEEE Trans. Power Electron.*, vol. 26, no. 9, pp. 2414–2425, Sep. 2011.

[7] V. Khadkikar, "Enhancing electric power quality using UPQC: A comprehensive overview," *IEEE*

Trans. Power Electron., vol. 27, no. 5, pp. 2284–2297, May 2012.

[8] L. G. B. Rolim, "Custom power interfaces for renewable energy sources," in *Proc. IEEE ISIE*, 2007, pp. 2673–2678.

[9] N. Voraphonpipit and S. Chatratana, "STATCOM analysis and controller design for power system voltage regulation," in *Proc. IEEE/PES Transmiss. Distrib. Conf. Exhib.—Asia Pac.*, 2005, pp. 1–6.

[10] J. J. Sanchez-Gasca, N. W. Miller, E. V. Larsen, A. Edris, and D. A. Bradshaw, "Potential benefits of STATCOM application to improve generation station performance," in *Proc. IEEE/PES Transmiss. Distrib. Conf. Expo.*, 2001, vol. 2, pp. 1123–1128.

[11] A. P. Jayam, N. K. Ardesna, and B. H. Chowdhury, "Application of STATCOM for improved reliability of power grid containing a wind turbine," in *Proc. IEEE Power Energy Soc. Gen. Meet.—Convers. Del. Elect. Energy 21st Century*, 2008, pp. 1–7.

[12] C. A Sepulveda, J. A Munoz, J. R. Espinoza, M. E. Figueroa, and P. E. Melin, "All-on-chip dq-frame based D-STATCOM control implementation in a low-cost FPGA," *IEEE Trans. Ind. Electron.*, vol. 60, no. 2, pp. 659–669, Feb. 2013.

[13] B. Singh and S. R. Arya, "Back-propagation control algorithm for power quality improvement using DSTATCOM," *IEEE Trans. Ind. Electron.*, vol. 61, no. 3, pp. 1204–1212, Mar. 2014.

[14] M. Aredes and R. M. Fernandes, "A dual topology of unified power quality conditioner: The iUPQC," in *Proc. EPE Conf. Appl.*, 2009, pp. 1–10.

[15] M. Aredes and R. M. Fernandes, "A unified power quality conditioner with voltage sag/swell compensation capability," in *Proc. COBEP*, 2009, pp. 218–224.

[16] B. W. Franca and M. Aredes, "Comparisons between the UPQC and its dual topology (iUPQC) in dynamic response and steady-state," in Proc. 37th IEEE IECON, 2011, pp. 1232–1237.

[17] B. W. Franca, L. G. B. Rolim, and M. Aredes, "Frequency switching analysis of an iUPQC with hardware-in-the-loop development tool," in Proc. 14th EPE Conf. Appl., 2011, pp. 1–6.

[18] B.W. Franca, L. F. da Silva, and M. Aredes, "Comparison between alphabeta and DQ-PI controller applied to IUPQC operation," in Proc. COBEP, 2011, pp. 306–311.

[19] R. J. Millnitz dos Santos, M. Mezaroba, and J. C. da Cunha, "A dual unified power quality conditioner using a simplified control technique," in Proc. COBEP, 2011, pp. 486–493.

[20] Y. Tang et al., "Generalized design of high performance shunt active power filter with output LCL filter," IEEE Trans. Ind. Electron., vol. 59, no. 3, pp. 1443–1452, Mar. 2012. [21] H. Akagi, E. Watanabe, and M. Aredes, Instantaneous Power Theory and Applications to Power Conditioning. New York, NY, USA:Wiley-IEEE Press, 2007.

[22] J. M. Guerrero, P. C. Loh, T.-L. Lee, and M. Chandorkar, "Advanced control architectures for intelligent micro grids—Part II: Power quality, energy storage, and AC/DC micro grids," IEEE Trans. Ind. Electron., vol. 60, no. 4, pp. 1263–1270, Apr. 2013.

[23] S. R. Bowes and S. Grewal, "Novel harmonic elimination PWM control strategies for three-phase PWM inverters using space vector techniques," Proc. Inst. Elect. Eng.—Elect. Power Appl., vol. 146, no. 5, pp. 495–514, Sep. 1999.

[24] M. Liserre, R. Teodorescu, and F. Blaabjerg, "Multiple harmonics control for three-phase grid converter systems with the use of PI-RES current

controller in a rotating frame," IEEE Trans. Power Electron., vol. 21, no. 3, pp. 836–841, May 2006.

[25] R. Teodorescu, F. Blaabjerg, U. Borup, and M. Liserre, "A new control structure for grid-connected LCL PV inverters with zero steady-state error and selective harmonic compensation," in Proc. 19th Annu. APEC Expo., 2004, vol. 1, pp. 580–586.

[26] X. Yuan, W. Merk, H. Stemmler, and J. Allmeling, "Stationary-frame generalized integrators for current control of active power filters with zero steady-state error for current harmonics of concern under unbalanced and distorted operating conditions," IEEE Trans. Ind. Appl., vol. 38, no. 2, pp. 523–532, Mar./Apr. 2002.

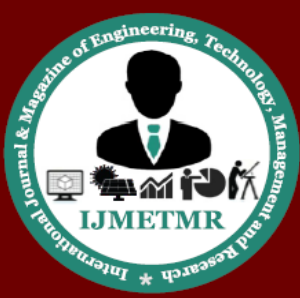
[27] D. N. Zmood and D. G. Holmes, "Stationary frame current regulation of PWM inverters with zero steady-state error," IEEE Trans. Power Electron., vol. 18, no. 3, pp. 814–822, May 2003.

[28] D. N. Zmood, D. G. Holmes, and G. H. Bode, "Frequency-domain analysis of three-phase linear current regulators," IEEE Trans. Ind. Appl., vol. 37, no. 2, pp. 601–610, Mar./Apr. 2001.

[29] M. Ciobotaru, R. Teodorescu, and F. Blaabjerg, "A new-single PLL structure based on second order generalized integrator," in Proc. 37th IEEE PESC, Jeju, Island, Korea, 2006, pp. 1–6.

[30] D. R. Costa, Jr., L. G. B. Rolim, and M. Aredes, "Analysis and software implementation of a robust synchronizing circuit based on pq theory," IEEE Trans. Ind. Electron., vol. 53, no. 6, pp. 1919–1926, Dec. 2006.

[31] M.K. Ghartemani, "A novel three-phase magnitude-phase-locked loop system," IEEE Trans. Circuits Syst. I, Reg. Papers, vol. 53, no. 8, pp. 1798–1802, Aug. 2006.



[32] M. S. Padua, S. M. Deckmann, G. S. Sperandio, F. P. Marafao, and D. Colon, "Comparative analysis of synchronization algorithms based on PLL, RDFT and Kalman filter," in Proc. IEEE ISIE, Jun. 2007, pp. 964–970.

[33] J. A. Moor Neto, L. Lovisolo, B. W. França, and M. Aredes, "Robust positive-sequence detector algorithm," in Proc. 35th IEEE IECON, Nov. 2009, pp. 788–793.

[34] V. Khadkikar, A. Chandra, A. O. Barry, and T. D. Nguyen, "Steady state power flow analysis of unified power quality conditioner (UPQC)," in Proc. ICIECA, 2005, pp. 1–6.

[35] V. Khadkikar, A. Chandra, A. O. Barry, and T. D. Nguyen, "Conceptual study of unified power quality conditioner (UPQC)," in Proc. IEEE Int. Symp. Ind. Electron., 2006, vol. 2, pp. 1088–1093.